

Article

# Experimental Research on Deformation Characteristics of Waste-Rock Material in Underground Backfill Mining

Pengfei Zhang <sup>1,2</sup> , Yubao Zhang <sup>1,2,3,\*</sup> , Tongbin Zhao <sup>1,2</sup>, Yunliang Tan <sup>1,2</sup> and Fenghai Yu <sup>1,2</sup>

<sup>1</sup> College of Mining and Safety Engineering, Shandong University of Science and Technology, Qingdao 266590, China; 15064221133@163.com (P.Z.); ztbwh2001@163.com (T.Z.); yunliangtan@163.com (Y.T.); yufenghai2006@163.com (F.Y.)

<sup>2</sup> State Key Laboratory of Mining Disaster Prevention and Control Co-founded by Shandong Province and the Ministry of Science and Technology, Shandong University of Science and Technology, Qingdao 266590, China

<sup>3</sup> School of Civil, Environmental and Mining Engineering, The University of Adelaide, Adelaide, SA 5005, Australia

\* Correspondence: zybsdust@163.com

Received: 2 January 2019; Accepted: 7 February 2019; Published: 11 February 2019



**Abstract:** Waste-rock material used in underground backfill mining has a granular texture and acquires non-linear deformation characteristics when compressed. The deformation modulus of waste-rock measured by a laboratory compression test is significantly different from the true deformation modulus in the field, due to the complete confining effect of the loading steel cylinder. In this study, we performed a series of laboratory-based compression tests on waste-rock samples. The results showed that lab-acquired deformation modulus variations of waste rock could be divided into three stages: slow increase, accelerated increase, and rapid increase. We also measured the true deformation modulus of backfill waste rock by conducting a field test in gob areas of the Tangshan coal mine, China. The hardening process of backfill waste rock during the field test was analyzed, and could be divided into four stages: roof contact, rapid compression, slow compression, and long-term stable. With the increase of axial strain, the lab- and field-measured deformation moduli of waste rock both increased exponentially. A correction parameter was proposed to investigate the relationship between the field-generated true deformation modulus and the lab-tested deformation modulus. The correction parameter  $k$  positively correlated with the axial strain, in the form of an exponential function. The magnitude of  $k$  was between 0.5616 and 0.6531.

**Keywords:** backfill mining; waste-rock material; deformation modulus; compression test; field test

## 1. Introduction

In recent years, backfill mining methods have developed rapidly around the world [1–4], among which waste-rock backfill mining has become increasingly popular in the Chinese coal mining industry [5–7]. This method not only protects surface buildings, but also reduces environmental pollution caused by the large quantities of waste-rock material produced during roadway excavations and coal washing [8–12]. However, the deformation characteristics of waste-rock materials greatly affect the roof stability by overlying the strata movement of gob areas, and consequently dominate surface subsidence [13–17]. The bearing capacity of backfilled waste-rock in gob areas is influenced by its deformation modulus. Therefore, it is of great significance to accurately and efficiently evaluate the deformation modulus of backfill waste-rock material in underground backfill mining.

Waste-rock is a type of granular material, with non-linear mechanical characteristics emerging during rock testing [18–22]. During large-scale direct shear tests, Lee et al. [23] found that the

stress–strain behavior of crushed rock is nonlinear, inelastic, and stress-dependent. Li et al. [24] performed a series of compression tests, which showed that waste-rock deformation was rather large in the initial portion of the compression test. Su et al. [25] conclude that the deformation process of crushed stones performed over time could be divided into three stages: rapid deformation, slow deformation, and stable deformation. Generally, the stress–strain characteristics of crushed waste-rock material are influenced by grain size, gradation, degree of saturation, uniformity, particle breakage, etc. Hu et al. [26] investigated the relationship between the compression ratio, lateral pressure, and particle gradation of waste-rock samples in a systematic series of compression tests. Li et al. [27] applied numerical simulation experiments to study the loading capacity and deformation response of filling particles under uniaxial compression. Ma et al. [28] indicate that the effective porosity of crushed limestone samples decreases with the decrease in bigger particle size. Using a self-designed bidirectional loading test system for granular materials, Li et al. [29] investigated the influence of lateral stress on the compaction deformation characteristics of crushed waste-rock samples. The deformation modulus measured by the above-mentioned laboratory tests is not a constant, but rather a nonlinear variable. While most compression tests are carried out under complete confinement conditions (zero lateral strain), this is not a common boundary condition of field waste-rock in a gob area [30–32]. The lateral boundary condition of waste-rock in a gob area is significantly vague and difficult to be represented exactly in a laboratory compression test. The deformation modulus of material is significantly different because of the different confining pressures [33–35]. Not surprisingly, there is a large error in the lab-measured deformation modulus compared to the true deformation modulus of waste-rock in a gob area. In addition, measuring the true deformation modulus of backfill waste-rock in gob areas is difficult, due to the complicated field conditions.

In this study, a series of laboratory-based compression tests were carried out on waste rock samples. The deformation modulus change law was analyzed based on lab test results. The true deformation modulus of backfill waste rock in gob areas was also measured during a field test performed in the Tangshan coal mine in China. The hardening process of backfill waste rock in the field was explored in detail. Finally, a correction parameter was proposed to investigate the relationship between the field-derived true deformation modulus and laboratory-tested deformation modulus. The feasibility and effectiveness of the correction parameter with axial strain were discussed.

## 2. Laboratory Compression Test

### 2.1. Preparation of Waste Rock Samples

In this study, the waste-rock material was directly sampled from the backfilling area of the F5001 working face in the Tangshan coal mine in China. After measurement, the initial physical and mechanical parameters are listed in Table 1. In order to determine the gradation of the original waste-rock particles, an experimental sieve was used to screen the waste-rock. The original particle gradation was obtained and shown in Figure 1.

**Table 1.** Physical and mechanical properties of waste-rock samples.

Parameter	Bulk Density (kg/m <sup>3</sup> )	Moisture Content (%)	Porosity (%)	Crushing Expansion
Measured value	1104	9.2	48.3	1.80

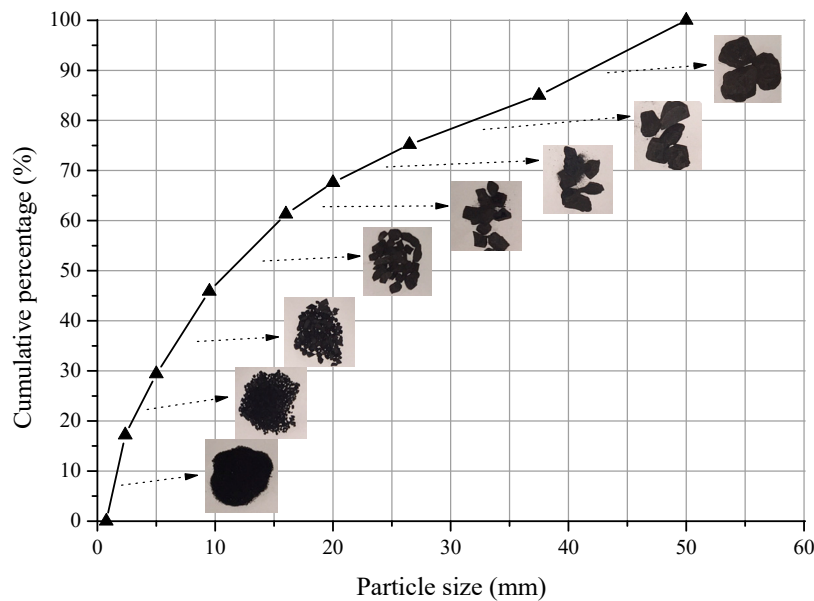


**Figure 1.** Size distribution of waste-rock particles.

As per the experimental requirements for compressing coarse-grained soil materials [16,29,36], the maximum particle size of the material was less than one-fifth of the inner diameter of the compression cylinder. In this study, the inner diameter of the compression cylinder was 100 mm, indicating a waste-rock maximum particle size of 20 mm. The particles gradation was designed based on the equivalent substitution method [37], where the content of over-sized materials is replaced by the weighted mean of coarse-grained particles with 5–20 mm diameter. The substituted grain percentage of waste-rock particles was calculated by Equation (1), and is listed in Table 2:

$$P_{5i} = \frac{P_5}{P_5 - P_0} P_{05i} \tag{1}$$

where  $P_5$  is the original content sum of waste-rock particles with a diameter larger than 5 mm (%);  $P_{5i}$  is the content of different particle sizes with a 5–20 mm diameter after calculation (%);  $P_{05i}$  is the original content of different particle sizes before calculation (%); and  $P_0$  is the content sum of over-sized waste-rock particles with a diameter larger than 20 mm (%).

**Table 2.** Gradation composition of treated waste-rock particles.

Particle Size (mm)	≤2.36	2.36~5	5~9.5	9.5~16	16~20
Percentage (%)	17.2	12.2	30.5	28.5	11.6

### 2.2. Experimental Scheme

The waste-rock compression test was carried out using the RLJW-2000 servo-controlled compressive testing equipment (Figure 2a). The equipment’s maximum axial force is 2000 kN. The most important part of the equipment is the loading system, which is composed of the steel cylinder, loading indenter, and base.

As shown in Figure 2b, the inner diameter of the steel cylinder is 100 mm, the outer diameter is 124 mm, and the depth is 230 mm. The radius and height of the matching loading indenter are 99 mm and 100 mm, respectively. The stiffness of the loading cylinder is 210 GPa, which is much larger than that of the waste-rock material. Therefore, the compression test can be considered to be under the condition of complete confinement (zero lateral strain). The waste-rock samples were mixed adequately and filled into the loading cylinder, and the filling height was 200 mm. The three groups

of waste-rock samples, which were made according to the gradation scheme in Table 2, were tested. The axial displacement and stress of waste-rock samples were recorded using an axial extensometer and testing machine, respectively. The loading mode was displacement control, and the loading rate was 0.25 mm/min.

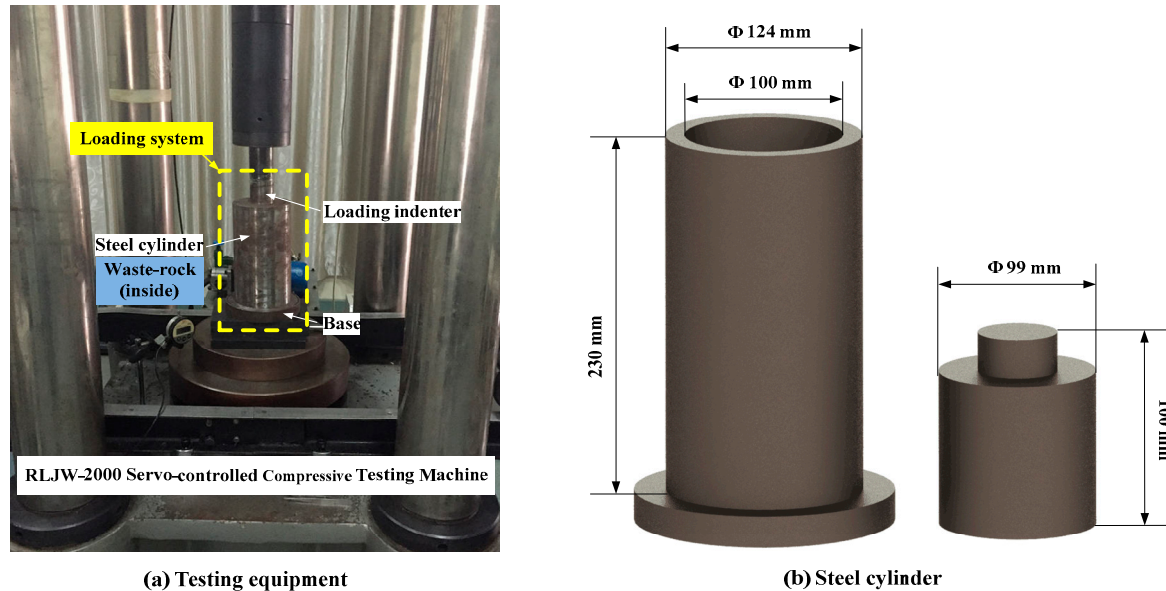


Figure 2. Testing system: (a) testing equipment; (b) steel cylinder.

### 2.3. Experimental Result

Figure 3 shows the deformation modulus and axial stress curves versus axial strain of the waste-rock sample. According to the increase rate of the deformation modulus curve, the change of deformation modulus could be divided into three stages (Figure 3):

(1) Slow increase stage: in this stage, the void surrounding coarse particles of the waste-rock sample is continuously compressed, and the samples' axial stress gradually increased, but the magnitude is small. The deformation modulus increase of the waste-rock sample is slow and almost linear.

(2) Accelerated increase stage: in this stage, waste-rock particles with lower strength are crushed and compacted, and the samples' axial stress (overall strength) increases quickly. As a result, the deformation modulus of the waste-rock sample increases acceleratingly at a higher rate.

(3) Rapid increase stage: in this stage, the waste-rock particles are completely compacted. Due to the complete confinement effect of the loading steel cylinder on the waste-rock sample, the deformation ability of the sample decreases, and the axial stress increases rapidly. Consequently, the deformation modulus of the waste-rock sample increases sharply.

It was clearly visible that the deformation modulus of the waste-rock sample increased exponentially with the increase in axial strain. The exponential equation for fitting the relationship between the deformation modulus and axial strain is as follows:

$$E_s = 6.5733 \cdot e^{18.53\epsilon} \quad (2)$$

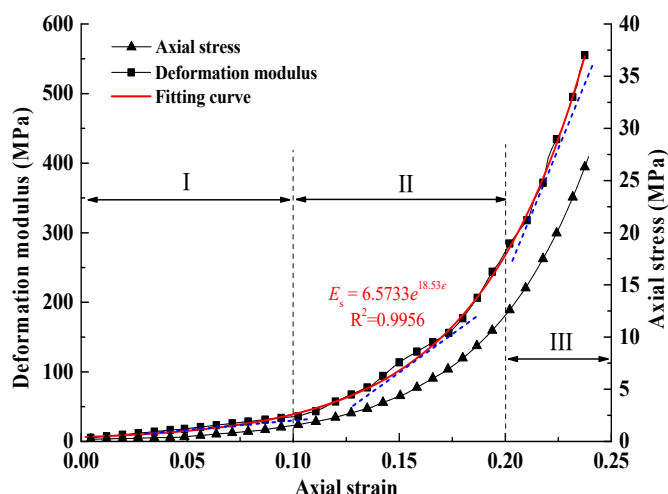


**Figure 3.** Experimental curves of the deformation modulus and axial stress vs. axial strain of the waste-rock sample.

### 3. Field Test on Backfill Waste Rock in Gob Areas

#### 3.1. Project Introduction

The F5001 mining working face is located in the 5# coal seam of the Tangshan coal mine (Hebei Province, China). The average dip angle and thickness of the 5# coal seam are 11° and 2.0 m, respectively. The F5001 working face adopts the longwall, fully mechanized strip-mining technique with backfill. The mining height and depth are 2.0 m and −660 m, respectively. The strike and dip dimensions of the F5001 mining face are 639.5 m and 66 m, respectively. Figure 4 shows the layout diagram of the F5001 working face. The filling system of the waste-rock material in the F5001 working face includes the surface waste-rock backfilling and feeding system, as well as the underground raw coal separation system (Figure 5). The waste-rock material is composed of two parts: underground washed waste rock and the surface washed waste rock. The surface washed waste rock was sent from the feeding bore hole to the gangue haulage roadway, and the underground washed waste rock was transported from the underground coal washing chamber to the gangue haulage roadway. After then, the two parts were transported together to the gob area through the gangue haulage roadway. The waste-rock material was dropped from the scraper conveyor and filled into the gob area by the compactor.

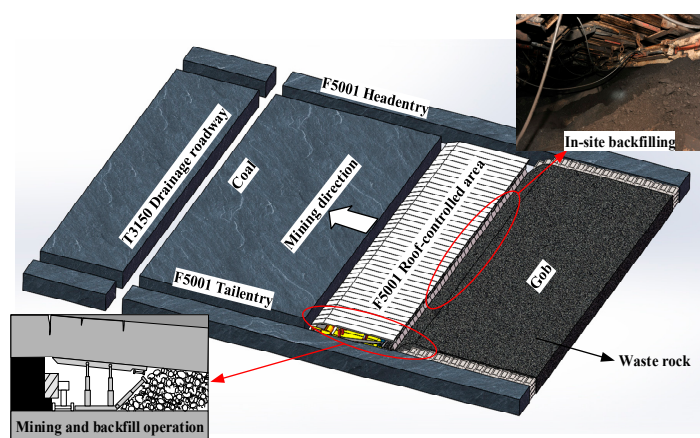


**Figure 4.** Layout diagram of the F5001 mining working face.

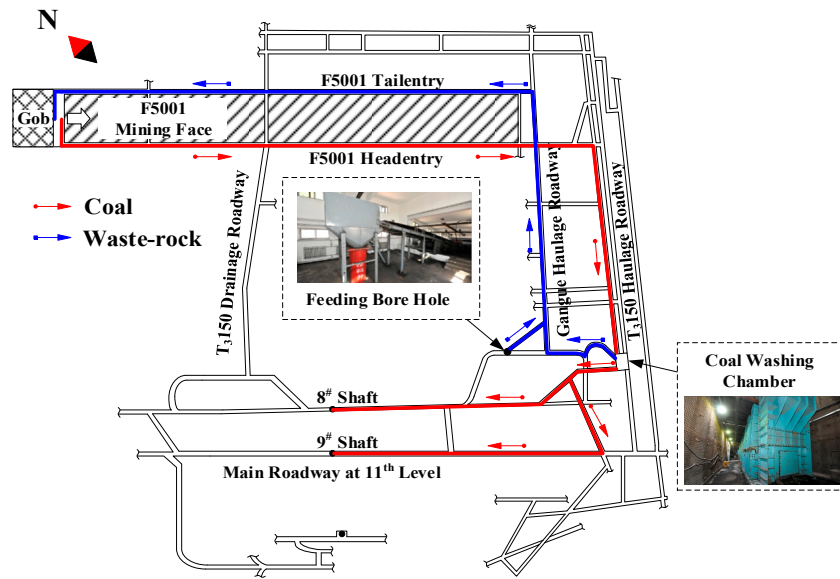


Figure 5. Transport route of waste-rock material and coal in underground mining.

3.2. Test Scheme

To determine the true deformation modulus of waste-rock material in gob areas, accurate measurements of the vertical displacement and backfill waste-rock stress were needed. The GUD500 displacement sensor and GPD30 stress sensor were used to monitor backfill waste-rock displacement and stress, respectively. The sensors were installed at the working face center, in the dip’s direction, and pre-buried in the roof-controlled safety zone behind the support (Figure 6). The sensors’ sampling frequency was 720 times per hour. The monitoring system was composed of sensors, transmission signal lines, hubs, communication master stations, monitoring sub-stations, a power supply, etc. [38,39] Data were continuously recorded for 45 days, during which the working face advanced 162 m.

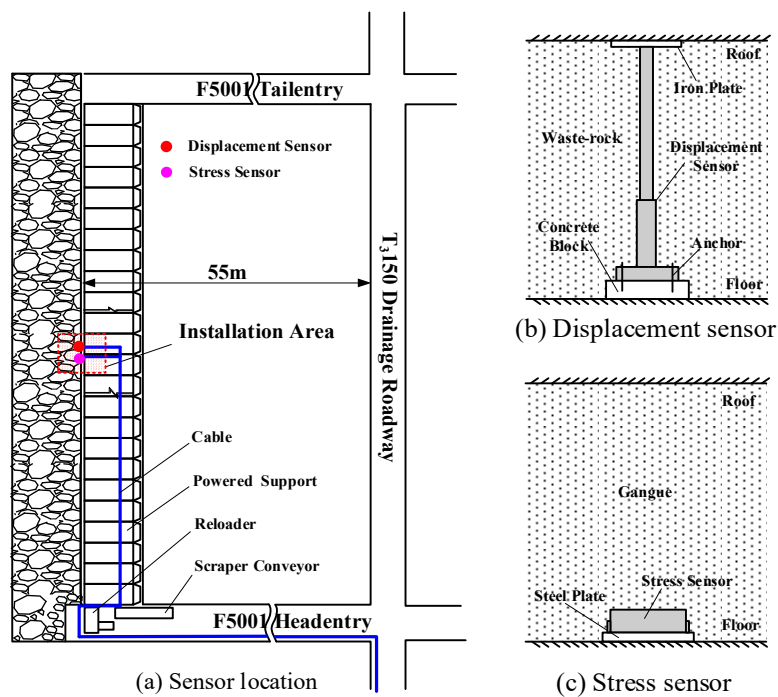


Figure 6. Layout of the waste-rock monitoring sensors in gob areas: (a) sensor location; (b) displacement sensor; and (c) stress sensor.

### 3.3. The Hardening Process of Waste Rock

Vertical displacement and stress monitoring curves of waste rock in gob areas are shown in Figures 7 and 8, respectively. When the working face's mining distance reached 160 m, the axial displacement of waste rock in gob areas reached a maximum of 425.50 mm, and the waste-rock stress reached a maximum of 2.87 MPa. The strong roof movement in gob areas during working face advancement causes a distinct hardening process in waste-rock material. As shown in Figures 7 and 8, the hardening process of waste rock in gob areas can be divided into four stages:

- (1) Roof contact stage: In this stage, the backfill waste rock is loose and not in complete contact with the roof in gob areas. The tamper machine continuously compacts waste rock in gob areas, resulting in low stress movement of waste-rock material. At this stage, the roof in gob areas bends down freely. When working face's mining distance reaches 10 m, the axial stress of waste rock begins to increase significantly, indicating contact between the waste-rock and roof in gob areas. It is worth mentioning that at this stage, displacement is just roof movement and not waste rock compression in gob areas.
- (2) Rapid compression stage: at the beginning of this stage, waste rock is compressed under the roof's vertical loading in gob areas, and the internal void or pores are gradually compacted. The axial displacement of the waste rock increases rapidly, and the stress value increases greatly. At this stage, the compression value of waste rock was 183.62 mm, and the stress increment was 1.88 MPa.
- (3) Slow compression stage: in this stage, the compressive displacement and stress of waste rock increases slowly, and the growth rates decrease to close to zero. This implies that the bearing capacity of waste rock grows gradually stronger, and that waste-rock material shows significant hardening characteristics. The displacement and stress increments of waste rock in this study were 56.02 mm and 0.64 MPa, respectively.
- (4) Long-term stable stage: at this stage, the waste rock's average displacement and stress growth rates were 0.20 mm/m and 0.0017 MPa/m, respectively. Waste-rock material in gob areas was completely compacted, and the compression displacement and stress values were basically constants.

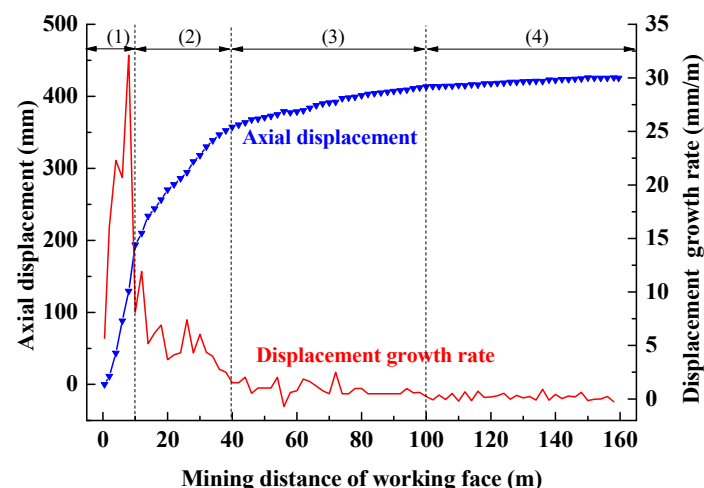


Figure 7. Axial compressive displacement and growth rate of waste rock.

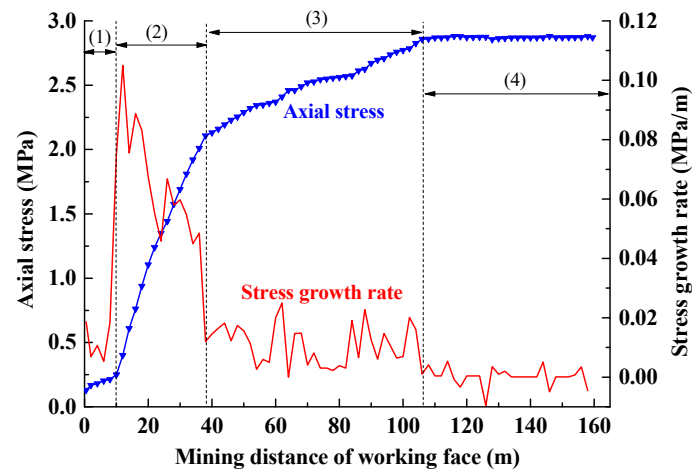


Figure 8. Axial stress and growth rate of waste rock.

### 3.4. Deformation Modulus of Waste Rock in the Field

Figure 9 shows the deformation modulus curve versus axial strain of the backfill waste rock in gob areas. As shown in Figure 9, when the axial strain was less than 0.10, the deformation modulus increased slowly, and data fluctuations were very small. However, when the axial strain was more than 0.10, the deformation modulus increased quickly in a continuous fluctuation. This corresponds to the third stage (slow compression stage) of the waste rock hardening process in gob areas. When the axial strain reached 0.143, the waste-rock became stable, and the deformation modulus no longer changed. As a whole, the deformation modulus was also increasing exponentially with the increase in axial strain. The fitting equation can be obtained as

$$E_g = 3.6915 \cdot e^{18.94\epsilon} \tag{3}$$

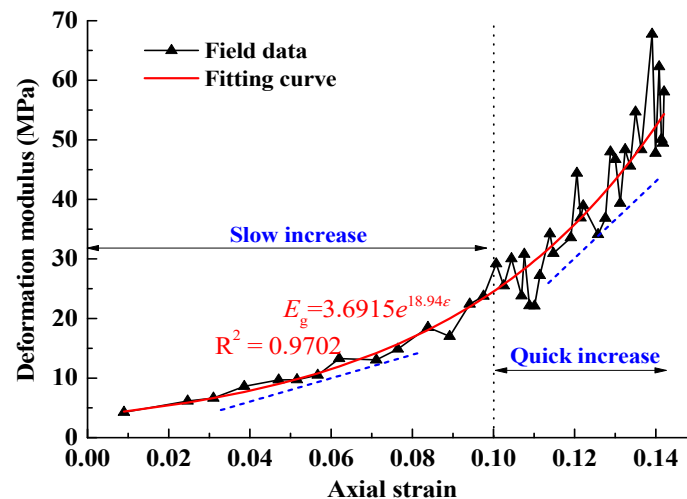


Figure 9. Deformation modulus vs. axial strain of waste rock in gob areas.

## 4. Discussions

### 4.1. Comparison of Results

The results of the laboratory- and field-based tests indicate that the two deformation moduli were related to the axial strain as an exponential function. As shown in Figure 9, the Stage I curve of deformation modulus increased slowly and fluently in the field test. It is close to the laboratory test results (Figure 3). Obviously, the Stage II curve increased faster than Stage I curve in Figure 9,

analogous to that in Figure 3. The maximum axial strain of waste rock in the gob area is only 0.143; however, the lab measured maximum axial strain at 0.24. Because the roof in the gob area reached stability after the working face advanced 100 m, the axial strain of waste rock would not increase. It is implied that the Stage III did not exist in the field-measured deformation modulus. In other words, the lab-measured deformation modulus is inaccurate, and not appropriate for application in underground backfill mining design.

The main reason for the difference between laboratory and field test results is that the tests are carried out under different lateral boundary conditions. In the laboratory test, under the complete lateral confinement condition, the volumetric strain of the waste-rock samples is equal to the axial strain. However, in the field test, under the incomplete lateral confinement condition, the volumetric strain is equal to the sum of the axial strain and the double of lateral strain. This is why the lab-measured deformation modulus of waste rock is larger than that measured by the field test.

In order to reduce the difference between the lab-tested and true deformation moduli of waste-rock in gob areas, a correction parameter  $k$  for the deformation modulus of backfill waste-rock was proposed as follows:

$$k = \frac{E_g}{E_s} \quad (4)$$

where  $E_s$  is the deformation modulus from the experimental test (MPa),  $E_g$  is the deformation modulus from the field measurement (MPa), and  $0 < k < 1$ .

When substituting Equations (2) and (3) into Equation (4), one obtains

$$k = 0.5616 \cdot e^{0.41\varepsilon} \quad (5)$$

According to Equation (5), the correction parameter for the deformation modulus of backfill waste-rock in gob areas can be plotted as shown in Figure 10. The correction parameter  $k$  positively correlates with the axial strain. The minimum value for the correction parameter was 0.5616, and the maximum value was 0.8462. Generally, the maximum axial strain of waste rock was less than 0.3 [40]; therefore, the value of the correction parameter was between 0.5616 and 0.6351. Considering the size effect of the lab-scale test and different engineering field conditions, the results are only applicable to the Tangshan coal mine in this study. However, the results could provide some guidance and references for similar backfill mining projects.

In addition, particle size and grading of waste rock played an important role in the deformation and strength of the waste-rock material [41–43]. Materials with strong resistance to deformation were obtained by adjusting the grading. Likewise, the correction parameter was greatly influenced by waste-rock particle grading. Without considering the axial strain, the better the particle grading, the greater the correction parameter, and the closer the correction parameter was to 1.0.

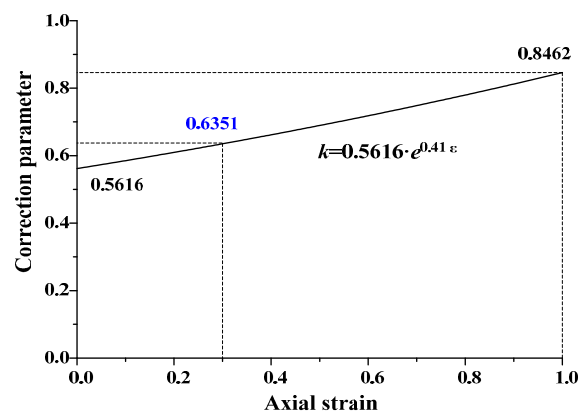


Figure 10. Correction parameter vs. axial strain.

#### 4.2. Numerical Verification

To verify the accuracy of the proposed correction parameter, the numerical model of backfilled mining was established based on the F5001 working face in the Tangshan coal mine. The axial strain and stress of the backfilled body in the numerical model were monitored, and the results were compared with the field measured values.

In the numerical simulation, firstly, the model was built according to the actual conditions of the working face, and the dimensions of the model were 196 m × 300 m × 100 m, as shown in Figure 11. Secondly, the Mohr–Coulomb model was chosen as the constitutive model of rocks, and the elastic model was adopted to simulate waste-rock material. The mechanical parameters of strata in the numerical simulation are listed in Table 3. As the axial strain changes, the deformation modulus of the waste rock increases exponentially, so it is necessary to continuously update the deformation modulus of the waste rock unit. Based on Equations (2) and (5), the true deformation modulus was calculated and updated using Fish language in FLAC3D. Then, the displacement boundary conditions of the bottom and around sides of the model were fixed. The axial stress with 16.5 MPa was applied on the top of the model, which was the ground stress of the mining working face. Finally, the working face was mined 10 m, and the waste-rock material was backfilled 10 m per each calculated circulation. Each calculated circulation was 2000 steps.

The simulation results are shown in Figures 12 and 13, and they are in good agreement with the field data. When the working face reached 160 m, the simulated axial displacement and stress of waste rock were 429.98 mm and 2.83 MPa, respectively. Their errors compared to the field data were 1.05% and 1.39%, respectively. In addition, the variation trend and magnitude of the simulated data were close to the field monitoring results. This indicates that the proposed correction parameter for the deformation modulus was feasible and valid, and the compression characteristics of field waste-rock can be displayed perfectly by this method.

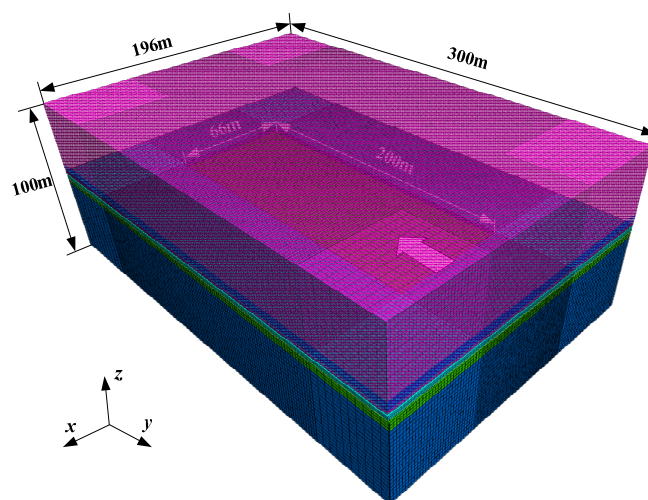


Figure 11. Numerical model in FLAC<sup>3D</sup>.

Table 3. The mechanical parameters of strata in the numerical simulation.

Position	Rock Type	Density/kg·m <sup>-3</sup>	Elastic Modulus/GPa	Poisson's Ratio	Frictional Angle/°	Cohesion/MPa	Tensile Strength/MPa
Main roof	sandy mudstone	2650	4.38	0.34	41	18.5	14
Immediate roof	mudstone	2300	2.34	0.30	38	9	8
5# Coal seam	coal	1340	1.19	0.33	26	3	1.4
Immediate floor	mudstone	2650	5.20	0.30	44	13	10
Main floor	siltstone	2650	4.38	0.34	41	18.5	14
Gob area	waste-rock	1100	3.69e <sup>-3</sup>	0.41	-	-	-

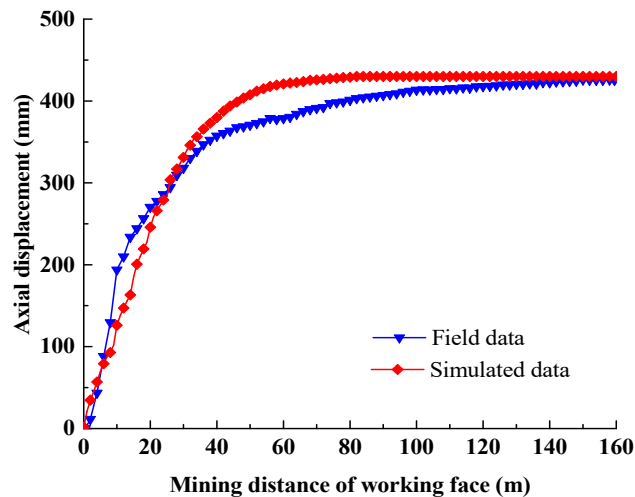


Figure 12. Contrast curves of the axial displacement of waste rock in gob areas.

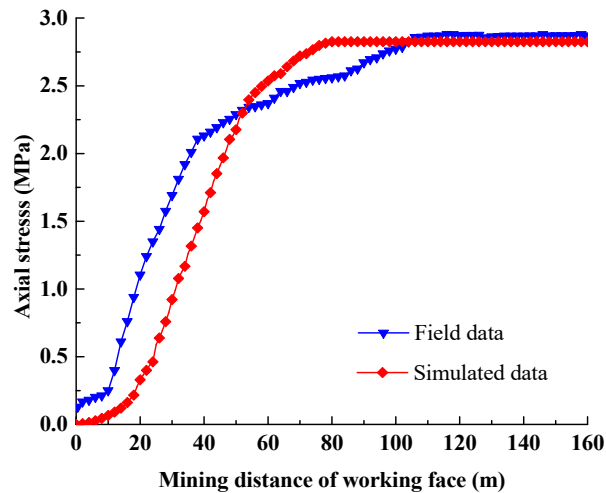


Figure 13. Contrast curves of axial stress of waste rock in gob areas.

## 5. Conclusions

- (1) A series of laboratory-based compression tests were carried out on waste-rock samples. In this context, the deformation modulus of waste rock increased exponentially with the increase in axial strain. The waste rock deformation modulus variation could be divided into three stages: low increase (stage I), accelerated increase (stage II), and rapid increase (stage III).
- (2) A field test was designed and performed to correctly measure the true deformation modulus of backfill waste rock in the Tangshan coal mine (Hebei Province, China). The axial displacement and stress of waste-rock were monitored for 45 days in a field-based test. It was found that the true deformation modulus was also increasing exponentially with the increase in axial strain. However, when the axial strain reached 0.143, it became stable and did not increase further. This was due to roof sinking stops and the overlying strata movement approaching equilibrium in gob areas.
- (3) The hardening process of backfill waste rock in the field test was analyzed and divided into four stages: roof contact, rapid compression, slow compression, and long-term stable stages. It is worth mentioning that the displacement at the roof contact stage was just the roof's movement, not the compression of backfill waste rock in gob areas.
- (4) Based on the results from the lab and field tests, a correction parameter for the true deformation modulus was proposed. The correction parameter  $k$  positively correlated with the axial strain in the form of an exponential function. The magnitude of  $k$  of waste-rock material in Tangshan

coal mine was between 0.5616 and 0.6351. By means of numerical verification, the correction parameter was used to calculate the true deformation modulus of waste rock, and this method provided some guidance and references for the design of underground backfill mining.

**Author Contributions:** T.Z. and Y.T. designed the theoretical framework; P.Z. and Y.Z. conducted the experiments and completed the numerical simulations; Y.Z. and F.Y. wrote the manuscript; P.Z. corrected the figures.

**Funding:** This research was supported by National Key R&D Program of China (2018YFC0604703), National Natural Science Foundation of China (No. 51704181), and China Scholarship Council (No. 201708370105).

**Acknowledgments:** The authors would like to thank the editors and the anonymous reviewers for their helpful and constructive comments.

**Conflicts of Interest:** The authors declare no conflict of interest.

## References

- Zhao, Y.; Soltani, A.; Taheri, A.; Karakus, M.; Deng, A. Application of slag-cement and fly ash for strength development of cemented paste backfills. *Minerals* **2019**, *9*, 22. [[CrossRef](#)]
- Zhang, J.; Deng, H.; Taheri, A.; Deng, J.; Ke, B. Effects of Superplasticizer on the Hydration, Consistency, and Strength Development of Cemented Paste Backfill. *Minerals* **2018**, *8*, 381. [[CrossRef](#)]
- Khaldoun, A.; Ouadif, L.; Baba, K.; Bahi, L. Valorization of mining waste and tailings through paste backfilling solution, Imiter operation, Morocco. *Int. J. Min. Sci. Tech.* **2016**, *26*, 511–516. [[CrossRef](#)]
- Benzaazoua, M.; Fall, M.; Belem, T. A contribution to understanding the hardening process of cemented pastefill. *Miner. Eng.* **2004**, *17*, 141–152. [[CrossRef](#)]
- Yin, Y.; Zou, J.; Zhang, Y.; Qiu, Y.; Fang, K.; Huang, D. Experimental study of the movement of backfilling gangues for goaf in steeply inclined coal seams. *Arab. J. Geosci.* **2018**, *11*, 318. [[CrossRef](#)]
- Zhang, J.X.; Zhou, N.; Huang, Y.L.; Zhang, Q. Impact law of the bulk ratio of backfilling body to overlying strata movement in fully mechanized backfilling mining. *J. Min. Sci.* **2011**, *47*, 73–84. [[CrossRef](#)]
- Zhang, J.X.; Zhang, Q.; Sun, Q.; Gao, R.; Germain, D.; Abro, S. Surface subsidence control theory and application to backfill coal mining technology. *Environ. Earth Sci.* **2015**, *74*, 1439–1448. [[CrossRef](#)]
- Lebre, E.; Corder, G.D.; Golev, A. Sustainable practices in the management of mining waste: A focus on the mineral resource. *Miner. Eng.* **2017**, *107*, 34–42. [[CrossRef](#)]
- Edraki, M.; Baumgartl, T.; Manlapig, E.; Bradshaw, D.; Franks, D.M.; Moran, C.J. Designing mine tailings for better environmental, social and economic outcomes: a review of alternative approaches. *J. Clean Prod.* **2014**, *84*, 411–420. [[CrossRef](#)]
- Yilmaz, E. Advances in reducing large volumes of environmentally harmful mine waste-rocks and tailings. *Gospod. Surowcami Miner.* **2011**, *27*, 89–112.
- Sun, W.; Wang, H.J.; Hou, K.P. Control of waste-rock-tailings paste backfill for active mining subsidence areas. *J. Clean Prod.* **2018**, *171*, 567–579. [[CrossRef](#)]
- Zhang, J.; Li, M.; Taheri, A.; Zhang, W.; Wu, Z.; Song, W. Properties and application of backfill materials in coal mines in China. *Minerals* **2019**, *9*, 53. [[CrossRef](#)]
- Wang, Y.; Taheri, A.; Xu, X. Application of Coal Mine Roof Rating (CMRR) in Chinese coal mines. *Int. J. Min. Sci. Tech.* **2018**, *28*, 491–497. [[CrossRef](#)]
- Karfakis, M.G.; Bowman, C.H.; Topuz, E. Characterization of coal-mine refuse as backfilling material. *Geotech. Geol. Eng.* **1996**, *14*, 129–150. [[CrossRef](#)]
- Yavuz, H. An estimation method for cover pressure reestablishment distance and pressure distribution in the goaf of longwall coal mines. *Int. J. Rock Mech. Min. Sci.* **2004**, *41*, 193–205. [[CrossRef](#)]
- Huang, P.; Spearing, A.J.S.; Feng, J.; Jessu, K.V.; Guo, S. Effects of solid backfilling on overburden strata movement in shallow depth longwall coal mines in west China. *J. Geophys. Eng.* **2018**, *15*, 2194–2208. [[CrossRef](#)]
- Tan, Y.L.; Liu, X.S.; Ning, J.G.; Lu, Y.W. In Situ Investigations on Failure Evolution of Overlying Strata Induced by Mining Multiple Coal Seams. *Geotech. Test. J.* **2017**, *40*, 244–257. [[CrossRef](#)]
- Zhang, J.X.; Huang, Y.L.; Li, M.; Zhang, Q.; Liu, Z. Test on mechanical properties of solid backfill materials. *Mater. Res. Innov.* **2014**, *18*, 960–965. [[CrossRef](#)]

19. Zhang, J.X.; Li, M.; Liu, Z.; Zhou, N. Fractal characteristics of crushed particles of coal gangue under compaction. *Powder Technol.* **2017**, *305*, 12–18. [[CrossRef](#)]
20. Taheri, A.; Tatsuoka, F. Small- and large-strain behaviour of a cement-treated soil during various loading histories and testing conditions. *Acta Geotech.* **2015**, *10*, 131. [[CrossRef](#)]
21. Taheri, A.; Sasaki, Y.; Tatsuoka, F.; Watanabe, K. Stress-strain relations of cement-mixed gravelly soil from multiple-step triaxial compression test results. *Soils Found.* **2012**, *52*, 748–766. [[CrossRef](#)]
22. Wang, C.; Deng, A.; Taheri, A. Three-dimensional discrete element modeling of direct shear test for granular rubber-sand. *Comput. Geotech.* **2018**, *97*, 204–216. [[CrossRef](#)]
23. Lee, D.-S.; Kim, K.-Y.; Oh, G.-D.; Jeong, S.-S. Shear characteristics of coarse aggregates sourced from quarries. *Int. J. Rock Mech. Min. Sci.* **2009**, *46*, 210–218. [[CrossRef](#)]
24. Li, M.; Zhang, J.; Gao, R. Compression characteristics of solid wastes as backfill materials. *Adv. Mater. Sci. Eng.* **2016**, 2496194. [[CrossRef](#)]
25. Su, C.D.; Gu, M.; Tang, X.; Guo, W.B. Experiment study of compaction characteristics of crushed stones from coal seam roof. *Chin. J. Rock Mech. Eng.* **2012**, *31*, 18–26. (In Chinese)
26. Hu, B.N.; Guo, A.G. Testing study on coal waste backfilling material compression simulation. *J. China. Coal. Soc.* **2009**, *34*, 1076–1080. (In Chinese)
27. Li, G.D.; Cao, S.G.; Li, Y.; Zhang, Z.Y. Load bearing and deformation characteristics of granular spoils under unconfined compressive loading for coal mine backfill. *Adv. Mater. Sci. Eng.* **2016**, 8530574. [[CrossRef](#)]
28. Ma, D.; Bai, H.B.; Miao, X.X.; Pu, H.; Jiang, B.Y.; Chen, Z.Q. Compaction and seepage properties of crushed limestone particle mixture: An experimental investigation for ordovician karst collapse pillar groundwater inrush. *Environ. Earth Sci.* **2016**, *75*, 1–14. [[CrossRef](#)]
29. Li, M.; Zhang, J.X.; Sun, K.; Zhang, S. Influence of lateral loading on compaction characteristics of crushed waste-rock used for backfilling. *Minerals* **2018**, *8*, 552. [[CrossRef](#)]
30. Zhang, Q.; Zhang, J.X.; Kang, T.; Sun, Q.; Li, W.K. Mining pressure monitoring and analysis in fully mechanized backfilling coal mining face-A case study in Zhai Zhen Coal Mine. *J. Cent. South Univ.* **2015**, *22*, 1965–1972. [[CrossRef](#)]
31. Sivakugan, N.; Widisinghe, S.; Wang, V.Z. Vertical stress determination within backfilled mine stopes. *Int. J. Geomech.* **2014**, *14*, 06014011. [[CrossRef](#)]
32. Yang, P.Y.; Li, L.; Aubertin, M. Stress ratios in entire mine stopes with cohesionless backfill: A numerical study. *Minerals* **2017**, *7*, 201. [[CrossRef](#)]
33. Guo, W.Y.; Tan, Y.L.; Yu, F.H.; Zhao, T.B.; Hu, S.C.; Huang, D.M.; Qin, Z. Mechanical behavior of rock-coal-rock specimens with different coal thicknesses. *Geomech. Eng.* **2018**, *15*, 1017–1027.
34. Liu, X.S.; Tan, Y.L.; Ning, J.G.; Lu, Y.W.; Gu, Q.H. Mechanical properties and damage constitutive model of coal in coal-rock combined body. *Int. J. Rock Mech. Min. Sci.* **2018**, *110*, 140–150. [[CrossRef](#)]
35. Tan, Y.L.; Yu, F.H.; Ning, J.G.; Zhao, T.B. Design and construction of entry retaining wall along a gob side under hard roof stratum. *Int. J. Rock Mech. Min. Sci.* **2015**, *77*, 115–121. [[CrossRef](#)]
36. GB/T 50123-1999: *Standard for Soil Test Method*; MWRPRC (Ministry of Water Resources of the People's Republic of China): Beijing, China, 1999. (In Chinese)
37. Fu, H.; Han, H.Q.; Ling, H. Effect of grading scale method on results of laboratory tests on rockfill materials. *Rock Soil Mech.* **2012**, *33*, 2645–2649. (In Chinese)
38. Zhao, T.B.; Zhang, Y.B.; Zhang, Z.Y.; Li, Z.H.; Ma, S.Q. Deformation monitoring of waste-rock- backfilled mining gob for ground control. *Sensors.* **2017**, *17*, 1044. [[CrossRef](#)]
39. Zhao, T.B.; Ma, S.Q.; Zhang, Z.Y. Ground control monitoring in backfilled strip mining under the metropolitan district: case study. *Int. J. Geomech.* **2018**, *18*, 05018003. [[CrossRef](#)]
40. Yan, H.; Zhang, J.X.; Zhou, N.; Zhang, S.; Dong, X.J. Shaft failure characteristics and the control effects of backfill body compression ratio at ultra-contiguous coal seams mining. *Environ. Earth Sci.* **2018**, *77*, 458. [[CrossRef](#)]
41. Wu, J.; Feng, M.; Xu, J.; Qiu, P.; Wang, Y.; Han, G. Particle size distribution of cemented rockfill effects on strata stability in filling mining. *Minerals* **2018**, *8*, 407. [[CrossRef](#)]
42. Li, J.; Huang, Y.; Chen, Z.; Li, M.; Qiao, M.; Kizil, M. Particle-crushing characteristics and acoustic-emission patterns of crushing gangue backfilling material under cyclic loading. *Minerals* **2018**, *8*, 244. [[CrossRef](#)]

43. Wu, J.; Feng, M.; Chen, Z.; Mao, X.; Han, G.; Wang, Y. Particle size distribution effects on the strength characteristic of cemented paste backfill. *Minerals* **2018**, *8*, 322. [[CrossRef](#)]



© 2019 by the authors. Licensee MDPI, Basel, Switzerland. This article is an open access article distributed under the terms and conditions of the Creative Commons Attribution (CC BY) license (<http://creativecommons.org/licenses/by/4.0/>).